Binary wave in a helical fiber

V. Krylov and L. I. Slepyan
Department of Solid Mechanics, Materials and Structures,
Faculty of Engineering, Tel Aviv University, 69978 Tel Aviv, Israel
(Received 11 November 1996; revised manuscript received 19 February 1997)

Axial dynamic tension of a flexible helical fiber is found to lead to a specific, extraordinary nonlinear wave consisting of two different portions. The leading portion is a quasiperiodical propagating wave with rotation opposite to the initial twist of the helix, while the rear portion is a sequence of standing waves rotating in the reverse direction. The interface is the origin of two angular-momentum fluxes which, being different in sign, fill up angular momenta of the leading and rear waves. The phenomenon described presents an interesting example of a zero-total-angular-momentum wave propagating in a twisted waveguide.
[S0163-1829(97)08021-1]

We consider an inextensible, flexible fiber of constant mass density ρ per unit length whose nonlinear vector equation of motion and inextensibility condition are, respectively,[1]

$$\frac{\partial}{\partial s}\left[F(s,t)\frac{\partial \mathcal{R}(s,t)}{\partial s}\right]=\rho\frac{\partial^2 \mathcal{R}(s,t)}{\partial t^2},\quad \left|\frac{\partial \mathcal{R}}{\partial s}\right|=1. \qquad (1)$$

Here, F is a non-negative internal tension force, $\mathcal{R}$ is the position vector, s is the coordinate aligned with the fiber, and t is time.

There is a large body of works devoted to the nonlinear dynamics of inextensible fibers and elastic strings. For an extended reference and historical notes see, for example, Ref. 2. An exact analytical solution describing solitary waves in an inextensible, infinite helical fiber was obtained in Ref. 4, some numerical results were presented in Ref. 5. Then this solution was extended for the case of an extensible string of an arbitrary nonlinear elastic material.[6] The solitary wave is shown to exist for any subsonic velocity. Also it was shown that neglecting extensibility leads to a low-velocity asymptote of the solution for the corresponding extensible fiber. Thus the fiber can be considered as inextensible if the wave velocity is low in comparison with the sound velocity in the material. Next, different types of solitary waves in the helical string, rotating as a rigid body, were considered in Ref. 7. A complete traveling wave solution describing all possible types of periodical and solitary waves in an inextensible fiber was obtained in Ref. 8.

In the present work, in contrast to these steady-state, intrinsic waves, a transient wave arising under an axial external force is considered. Such a wave of necessity bears evidence of the intrinsic waves. However, it is a complex object which is characterized by the presence of different types of waves and by separation of axial rotations in different directions. The uncommonness of this wave is a consequence of the waveguide being twisted.

It may be mentioned that helicoidal systems are relevant to a wide variety of fields (deployable structures in spatial technology, tethered satellite systems,[9] textile yarn manufacturing processes, curvilinear fibers as reinforcements of composite materials,[10] mechanical properties of helical DNA molecules, etc.). Relating to the general problem of energy consumption of a structure under extension,[11] the original goal of the present problem consideration was to determine the ability of an inextensible helix to resist dynamic extension (by transferring the work of the axial tension force into kinetic energy of transversal vibrations).

The formulation adopted here prescribes that the end point of the fiber ($s=0$) subjected to the external axial force is held on the axis of the helix (x axis); it is connected with the main, helical portion of the fiber, Fig. 1(a). The length of the helix under consideration is chosen to be large enough to eliminate a detectable reflection. The problem is studied numerically using the simplest discrete analogue of the continuous fiber. It is a chain of masses connected to each other by inextensible, massless links. The finite difference method of the first order with respect to time (the explicit scheme) is used. The accuracy of the scheme used was shown to be very high. In spite of the simplicity of the model, it is very effective for calculations and leads to good agreement with the exact analytical results.[12,5]

The wave formed under the conditions considered is shown in Figs. 2 and 3. This ''binary'' wave consists of two portions: the leading, quasiperiodical, propagating wave and the rear, standing wave, Fig. 2(b). These waves possess axial rotations in opposite directions: the leading wave untwists the helix, whereas the rear wave twists it. This phenomenon arises for two reasons: there is an initial twist in the waveguide that leads to a wave with rotation, and there is no external moment, and therefore the total angular momentum of the binary wave remains at zero. The wave is characterized by two different velocities which correspond to the leading, high-speed wave front and the low-speed interface as a short transient region which separates these two different waves. So, the wave as a whole is transient and consists of two totally different parts. At the same time, the structure of each part is in good accordance with the exact solutions for the steady-state waves in the corresponding infinite helix: solitary, periodical, and constant-force nonlinear traveling and standing waves.

To show this we present the appropriate analytical results. First of all we note that under a constant internal force, F, Eq. (1) is satisfied by the D'Alembert solution: $\mathcal{R}$

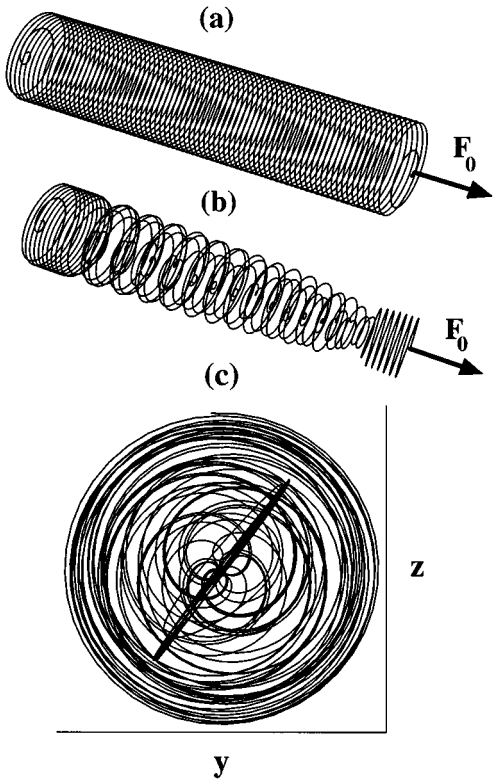

FIG. 1. (a) Initial shape of the fiber. The suddenly applied axial force F_0 acts at the point $s=0$ which is held on the axis of the helix. (b) Shape of the deformed helix. The helix is shown compressed: the length-to-radius ratio considered in the calculation is 200 times more. Three domains are shown (from the left to the right): undisturbed helix, leading wave, and rear, polarized wave. (c) Axial view of the deformed helix. The polarization of the rear wave is visible.

$=\mathcal{R}(s\pm c_0 t), c_0=\sqrt{F/\rho}$, where $\mathcal{R}$ is an arbitrary vector function which satisfies the extensibility condition in Eq. (1). The nontrivial wave solution of Eqs. (1) corresponds to a variable (propagating) internal force. This solution obtained in Refs. 4 and 8 is based on the representation of the position vector $\mathcal{R}(s,t)$ as the sum of a longitudinal vector $\boldsymbol{R}_x(s,t)$ and a vector $\boldsymbol{R}_\perp(s,t)$ lying in the cross section of the helix:

$$\boldsymbol{R}_x(s,t)=R_x(s,t)\boldsymbol{k}=[s\cos\gamma+u(\xi)]\boldsymbol{k},$$

$$R_\perp(s,t)=R(\xi)\exp(i\phi), \tag{2}$$

where $\phi=\lambda s/R_0+\omega t+\theta(\xi), \lambda=\sin\gamma, \xi=s-vt$, the unit vector $\boldsymbol{k}$ is directed along the x axis, γ is the angle between the fiber in its initial helical state and the x axis; v is the wave velocity along the fiber, and R_0 is the radius of the undeformed helix. Note that the complex representation of the rotating vector $\boldsymbol{R}_\perp$ (2) was shown in Ref. 3 to permit a traveling wave solution for the corresponding plane problem (an infinite ''helix'' with zero pitch was considered).

The representation of the position vector (2) permits system (1) to be reduced to a system of ordinary differential equations with respect to four unknown real functions $u(\xi), R(\xi), \phi(\xi)$, and $F(\xi)$. The integration of this system leads to the traveling wave solution, which includes solitary[4]

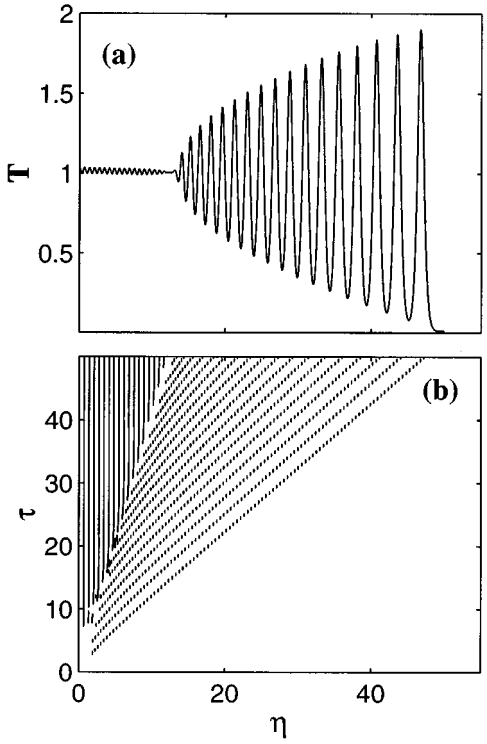

FIG. 2. (a) Normalized tension force. The ratio $T=F/F_0$ as a function of $\eta=\lambda s/(2\pi R_0)$ is shown. (b) Propagation of local peaks of the internal tension force. The quasifront and the interface propagating with different velocities $[\tau=\lambda c_1 t/(2\pi R_0)]$ are visible. The number of local peaks in the first wave is equal to that in the second wave.

and periodic[8] waves. The periodic cnoidal wave which propagates along the fiber with velocity v, can be defined by two parameters, say, maximal, $F_{\max}$, and minimal, $F_{\min}$, internal tension. The period of the wave is expressed as follows:[8]

$$L=\frac{2\sqrt{2}}{|\sigma|}R_0\left(\frac{1+f_{\min}}{\sqrt{f_{\min}+f_{\max}}}\boldsymbol{K}(k)-\sqrt{f_{\min}+f_{\max}}\boldsymbol{E}(k)\right)\times\operatorname{sgn}(F-\rho v^2), \tag{3}$$

where $\sigma=\lambda(1+c_0/v), f=F/(\rho v^2)$; $\boldsymbol{K}(k)$ and $\boldsymbol{E}(k)$ are complete elliptic integrals of the first and of the second kind, respectively, with parameter $k=(F_{\max}-F_{\min})^{1/2}(F_{\max}+F_{\min})^{-1/2}$. Note that the propagation of the wave along the fiber causes its rotation around the x axis and the wave possesses not only linear, but also angular momentum. In the case of the solitary wave the axial displacement and the internal force are as follows:[4]

$$u=(R-R_0)\cos\gamma, \quad F=\rho v^2\lambda^2/2(1-R^2R_0^{-2}). \tag{4}$$

We can now compare the structure and velocity of the leading quasiperiodical wave as well as the interface velocity with the relevant analytical results. The wave front velocity, v_1, as the velocity of the first peak of the wave, is nothing but the velocity c_1 of the solitary wave of the same amplitude [see Fig. 2 and formula (4)]. The first peak amplitude tends to $2F_0$, and using this formula the wave front velocity

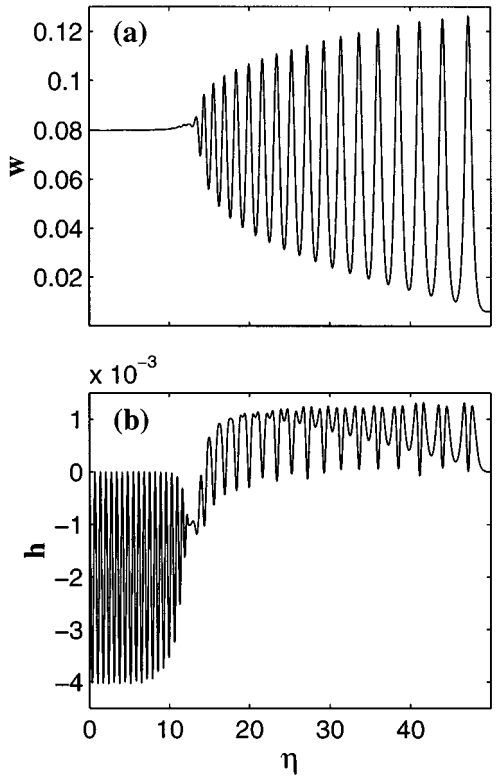

FIG. 3. (a) Normalized axial velocity, $w=\dot{u}/c_1$. (b) Normalized angular momentum, $h=R^2\dot{\phi}\lambda/(2\pi R_0 c_1)$. Two different waves which rotate in opposite directions are visible.

can be expressed in terms of the applied force as follows: $v_1 \sim c_1 = 2/\sin\gamma\sqrt{F_0/\rho}$. The quasiperiodical leading wave can be described locally by the traveling wave solution: the relation between the velocity of each peak, the minimal and the maximal forces, and the distance between two neighboring peaks are in accordance with that defined by Eq. (3), Fig. 4.

Two waves are separated by a short transient region. Within this region the internal force, F, remains almost constant, $F \sim F_0$, and the ''interface'' propagates with the

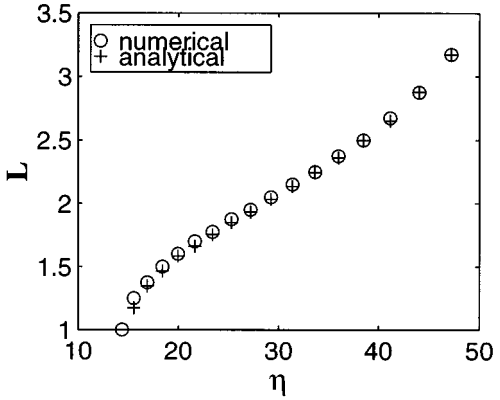

FIG. 4. Comparison of the local ''wavelength'' L as the distance between two neighboring peaks, in the leading wave, with the analytical results given by Eq. (3), $l=\lambda L/(2\pi R_0)$.

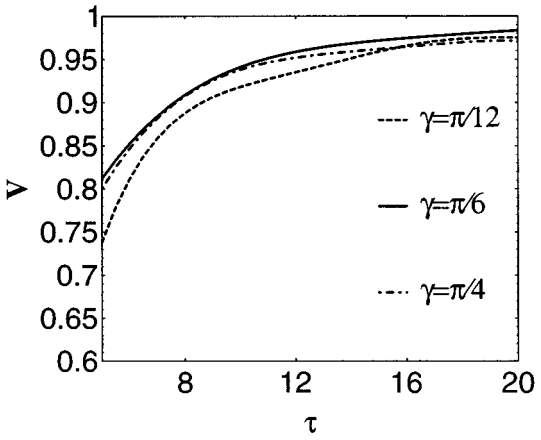

FIG. 5. Normalized wave front velocity, $V=v_1/c_1$ as a function of $\tau=\lambda c_1 t/(2\pi R_0)$.

D'Alembert wave velocity $v_2 \sim c_0 = \sqrt{F_0/\rho}$. Note that the structure of the wave is formed in time, and the above-written relations should be considered in the asymptotic sense. The results presented here differ from the limiting values by 2–3%. The establishment of the wave front velocity, v_1, in the ''pitch-of-the-helix-associated'' time, $\tau = \lambda c_1 t/(2\pi R_0)$, is shown in Fig. 5. In the τ scale, the tendency rate of v_1 to the velocity c_1 of the corresponding solitary wave is independent of the pitch of the helix.

Consider now the second wave. It consists of standing waves which do not propagate along the fiber. At the same time, the rear wave as a whole propagates along the fiber: there is a phase transition from the first, quasi-periodical wave mode to the second, standing wave mode. The rear wave appears to be almost completely polarized in a rotating plane, Figs. 1(b) and 1(c). This wave can also be locally described by an analytical solution. The standing wave solution can be obtained in the same way as the traveling wave solution.[4] In Eq. (2) put $\boldsymbol{R}_x(s,t)=R_x(s)\boldsymbol{k}, R(\xi) = R(s), \phi(t)=\omega t$. Substituting this representation into Eq. (1) and taking into account the boundary relation $F_0 = F(0)\boldsymbol{R}'\boldsymbol{k} = F(0)R_x'(0)$ one obtains

$$R_x' = F_0/F, \quad R' = \sqrt{F^2 - F_0^2}/F. \tag{5}$$

As a result of the integration of Eq. (1) [with Eq. (5) taken into account] we obtain

$$F = F_{\max} - \rho\omega^2 R^2/2, \quad R_{\max} = \sqrt{2/(\rho\omega^2)}\sqrt{F_{\max} - F_0}, \tag{6}$$

where $F_{\max}$ and $F_{\min}=F_0$ are minimal and maximal values of the tension. Integration of Eqs. (5) and (6) yields the $R-s$ relation in terms of elliptic functions and permits the wavelength to be found as a distance between two points $R=0$ as a function of two parameters, say $F_{\max}$ and ω. Note that the solution described can be obtained formally from the general traveling wave solution,[8] if we put $v \equiv 0, \lambda \equiv 0$. In this case, the wavelength is defined by Eq. (3). Calculations show that the numerical results are in good agreement with expressions (5) and (6): the difference does not exceed 0.5% (the calculations were performed for $\gamma=\pi/6$ with 80 nodes at pitch of the helix).

Expressions (5) and (6) can be essentially simplified. The tension force in the second wave is almost constant and asymptotic relations can be written down describing this wave, using small parameter $\mu=(F_{\max}-F_0)/F_0 \ll 1$. One can find

$$\frac{R}{R_{\max}} \sim \sin\left(\frac{\omega s}{\sqrt{F_0}}\right), \quad L \sim \frac{\pi\sqrt{F_0}}{\omega}, \quad \frac{R_{\max}}{L} \sim \frac{\sqrt{2\mu}}{\pi}. \quad (7)$$

Dynamic extension of a helix is also of interest in connection with the general problem of energy consumption of a structure by transferring the external force work into kinetic energy.[11] In this sense, the relation between the applied force and axial velocity of the end point of the helix (as the rate of its extension) is important. A rough analytical estimation of this relation (which is γ dependent) is derived below.

It follows from Eqs. (5)–(7) that the ''stretch'' of the helix, u', in the second wave almost reaches the maximal value $1-\cos\gamma$ because the difference $|R_x'-1|=(F-F_0)/F \leqslant (F_{\max}-F_0)/F_0=\mu$ is negligible, Fig. 2(a). Thus we assume that, in the second wave, $u'=u_2'=1-\cos\gamma$ that corresponds to the straight fiber [note that the helix in Figs. 1(a) and 1(b) is shown highly compressed]. Further the stretch of the helix in the first wave, averaged by the quasiperiod of the wave, is assumed to be a linear function of s (that is rather close to the results obtained):

$$u_1'=u_2'\frac{v_1t-s}{(v_1-v_2)t} \sim u_2'\frac{c_1t-s}{(c_1-c_0)t}, \quad s\in[v_2t,v_1t], \quad (8)$$

Now we can write down the required estimations of the displacement and velocity at the end point, $s=0$:

$$u_0=\int_0^{c_1t} u'\,ds = 1/2(\,1-\cos\gamma)(c_1+c_0)t,$$

$$v_0=\dot{u}_0=\sqrt{F_0}[1+(\sin\gamma)/2]\tan(\gamma/2). \quad (9)$$

The accuracy of the estimation Eq. (9) depends on γ. The estimation differs from the numerical results by 3% for $\gamma=\pi/12$, by 8% for $\gamma=\pi/6$ and by 25% for $\gamma=\pi/3$.

In conclusion, note that the same problem was considered for a plane, initially sinusoidal fiber. In this case, the structure of the wave looks like that of the leading wave in the helix. However, in this case there is no rotation, and the most interesting phenomenon considered as a separation of the wave into two parts does not take place: the rear standing wave does not arise at all.

This research was supported by Grant No. 94-00349 from the United States–Israel Binational Science Foundation (BSF), Jerusalem, Israel, Grant No. 9673-1-96 from the Ministry of Science, Israel, and by Colton Foundation, USA.

[1] H.F. Weinberger, *A First Course in Partial Differential Equations* (Blaisdell, New York, 1965).
[2] S.S. Antman, *Nonlinear Problems of Elasticity* (Springer-Verlag, New York, 1995), and references therein.
[3] P. Rosenau, Physica D **27**, 224 (1987), and references therein.
[4] L.I. Slepyan, V.I. Krylov, and R. Parnes, Phys. Rev. Lett. **74**, 2725 (1995).
[5] L.I. Slepyan, V.I. Krylov, and R. Parnes, Proc. Estonian Acad. Sci. Phys. Math. **44**, 29 (1995).
[6] L.I. Slepyan, V.I. Krylov, and Ph. Rosenau (unpublished).
[7] V.I. Krylov and Ph. Rosenau, Phys. Lett. A **217**, 31 (1996).
[8] V.I. Krylov, R. Parnes, and L.I. Slepyan (unpublished).
[9] V. Beletsky and E. Levin, *Dynamics of Space Tether Systems* (Nauka, Main Editorial Board for Physical and Mathematical Literature, Moscow, 1990).
[10] T.-W. Chou, *Microstructural Design of Fiber Composites* (Cambridge University Press, Cambridge, 1992).
[11] A.V. Cherkaev and L.I. Slepyan, Int. J. Damage Mech. **4**, 58 (1995).
[12] H. Wilson and K. Deb, Int. J. Nonlinear Mech. **27**, 795 (1992), and references therein.